

Reaction of CH₂ with adsorbed O on Ru(001) surface

A. Kis, J. Kiss, F. Solymosi *

*Institute of Solid State and Radiochemistry, University of Szeged,
and Reaction Kinetics Research Group of the Hungarian Academy of Sciences¹, P.O. Box 168, H-6701 Szeged, Hungary*

Received 15 January 2000; accepted for publication 30 March 2000

Abstract

The reaction pathways of CH₂ in the presence of coadsorbed oxygen atoms on Ru(001) surface were investigated by means of temperature-programmed desorption (TPD), photoelectron spectroscopy (XPS and UPS) and work function measurements. CH₂ species were produced by thermal and photoinduced dissociation of CH₂I₂. Preadsorbed oxygen atoms markedly stabilized C–I bonds, shifted the desorption of CH₂I₂ to higher temperatures and reacted with CH₂ formed to give formaldehyde above 200 K. Adsorbed formate was also detected in the temperature range of 300–450 K. The oxidation of surface species (CH₂O, HCOO, C_xH_y) proceeded above 450 K, to produce CO, CO₂, and H₂O. Illumination of the (CH₂I₂+O) coadsorbed layer initiated the dissociation of CH₂I₂, and induced the reaction of CH₂ with O slightly above 110 K. © 2000 Elsevier Science B.V. All rights reserved.

Keywords: Aldehydes; Oxygen; Photochemistry; Ruthenium; Thermal desorption spectroscopy; Ultraviolet photoelectron spectroscopy; Work function measurements; X-ray photoelectron spectroscopy

1. Introduction

The coupling and reactions of hydrocarbon fragments (CH₂, CH₃, C₂H₅, etc.) with adsorbed oxygen atoms represent important elementary steps in the selective and total oxidation of hydrocarbons and also in the reforming of methane to produce synthesis gas [1]. Previous works showed that CH₂ produced by the thermal and photodissociation of adsorbed CH₂I₂ on Pt(111) [2], Rh(111) [3–7] and Pd(100) [8] surfaces is readily combined with adsorbed oxygen atoms to give CH₂O which is released in the gas phase after its formation. Different results were obtained for Cu(100) [9].

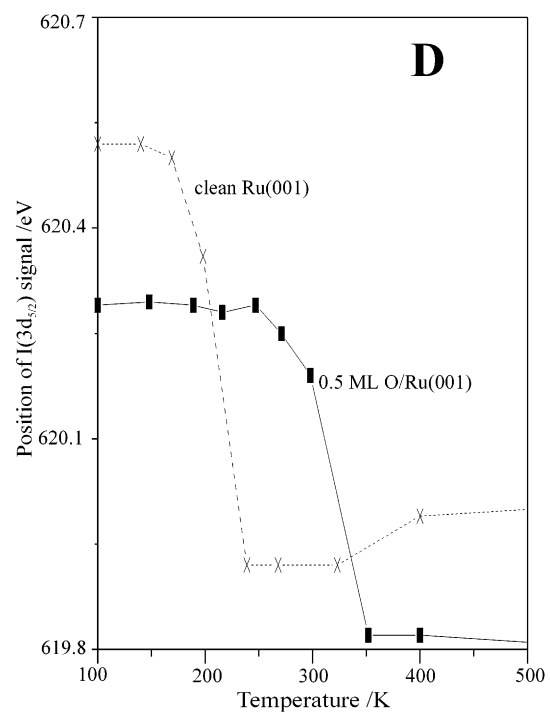
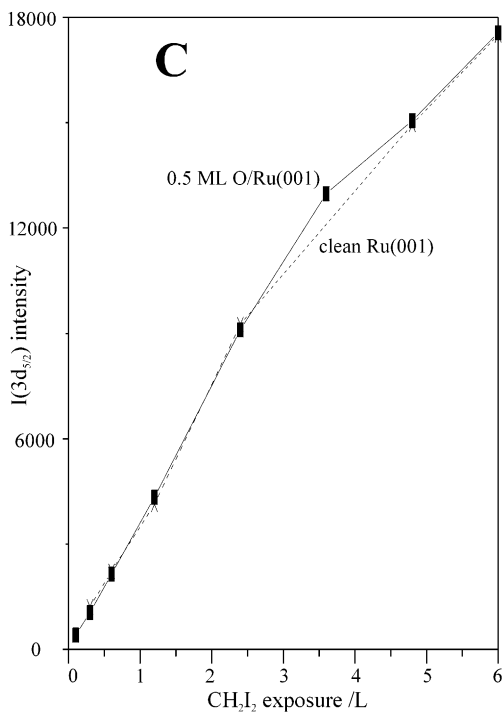
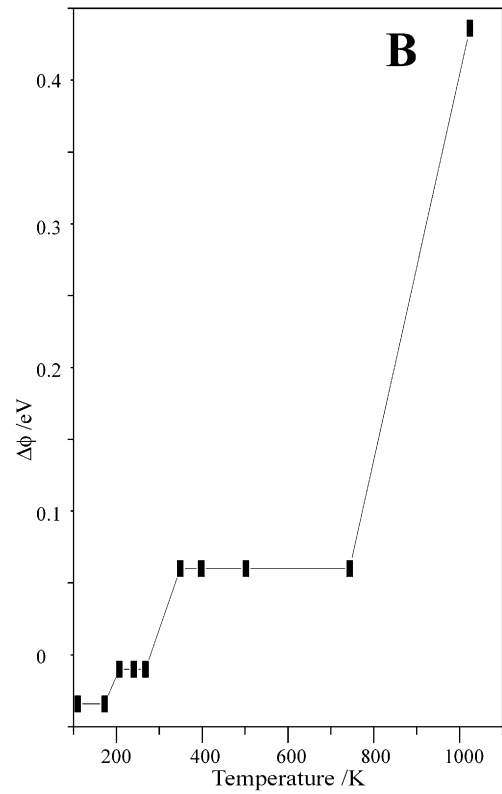
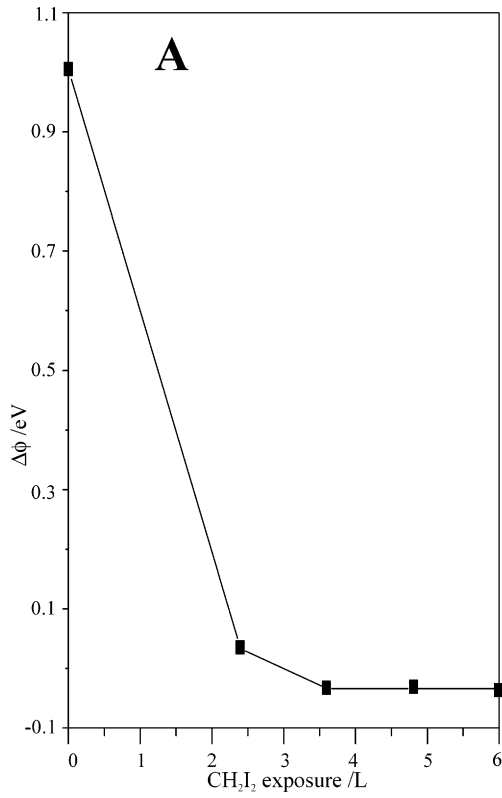
In this case adsorbed O did not alter the dominant pathways of the reaction of CH₂ formed above 200 K, e.g., the coupling of CH₂ into C₂H₄. Formaldehyde formation was observed only when CH₂ was produced at 100 K by illumination of CH₂I₂+O/Cu(100) system.

In a previous paper we gave an account on the chemistry of CH₂I₂ on the Ru(001) surface [10]. The aim of the present work is to elaborate the primary interaction of adsorbed CH₂ with atomically adsorbed O on Ru(001) surface and to determine the routes of subsequent reactions in the coadsorbed layer. Unlike other platinum metals, Ru is an excellent catalyst for the synthesis of higher hydrocarbons, but it is markedly less active and selective in the production of oxygenated hydrocarbons. Therefore, it was interesting to see its effect on the coupling of CH₂ with O.

* Corresponding author. Fax: +36 62 322 378.

E-mail address: fsolym@chem.u-szeged.hu (F. Solymosi)

¹ This laboratory is a part of the Center for Catalysis, Surface and Materials Science at the University of Szeged.



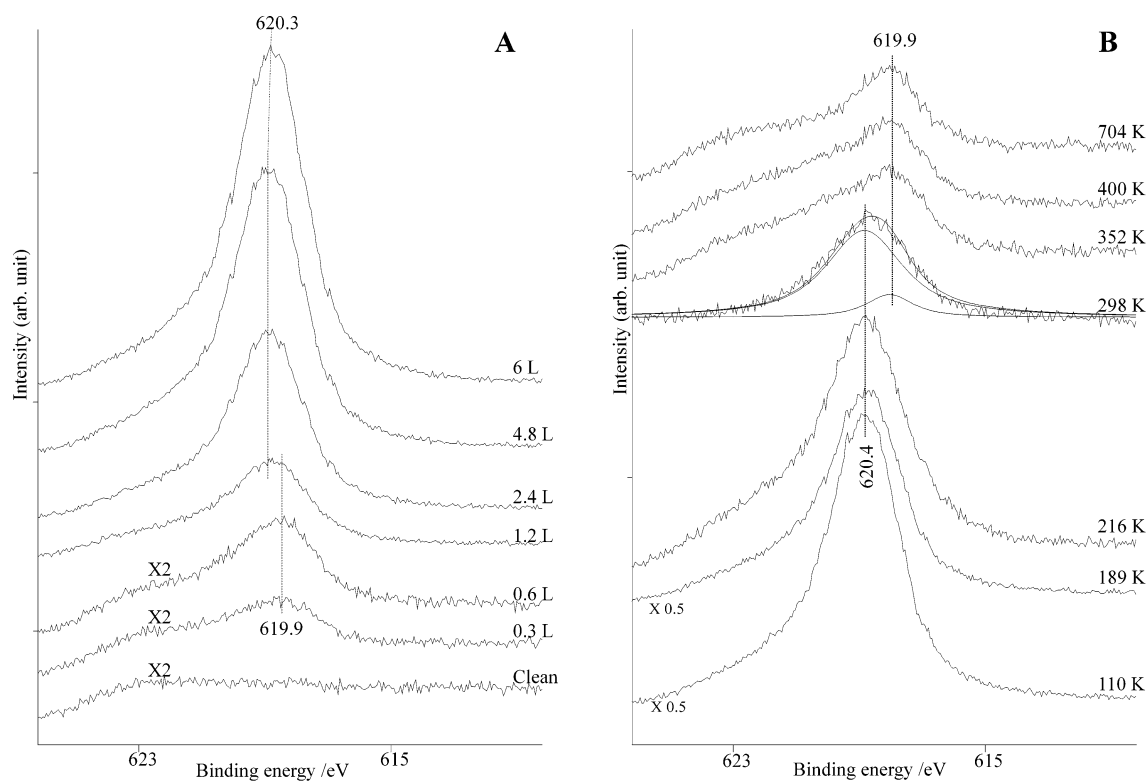


Fig. 2. (A) XPS spectra of Ru(001) as a function of CH_2I_2 adsorption at 100 K and (B) after heating the adsorbed layer to different temperatures. $\theta_{\text{O}}=0.5$. Exposure for (B) was 6 L.

2. Experimental

2.1. Methods

The experiments were performed in standard ultrahigh vacuum systems with a background pressure of 5×10^{-10} mbar produced by turbomolecular and ion-getter pumps. The chamber was equipped with an electrostatic hemispherical analyzer (Leybold-Heraeus LHS-10), a differentially pumped UV photon (He I, II) source for UPS, an X-ray source with Al anode for XPS and an electron gun for AES measurements. The directions of the UV source and electron analyzer with respect to the surface normal were 70° and 16° ,

respectively. All binding energies are referred to the Fermi level with the Ru $3d_{5/2}$ peak at 280.0 eV. Collection times for UPS and XPS were 15 and 30 min, respectively. XP spectra were smoothed by the fast Fourier transform method. For TPD, the sample was heated at 10 K s^{-1} from 110 K to a selected temperature. The mass spectrometer was in line of sight. Changes in work function were obtained by measuring the secondary electron cut-off in the He I UP spectra with the sample at -9 V relative to earth. The UV light source was a focused 40 W Hg lamp. The light passed through a high-purity sapphire window into the vacuum chamber. The incident angle was 30° off the surface normal.

Fig. 1. Changes in the work function ($\Delta\phi$) of O-dosed Ru(001) (A) as a function of CH_2I_2 exposure at 100 K and (B) annealing temperature. (C) Area of the iodine XPS signal at different CH_2I_2 exposure for clean and O-dosed Ru(001). (D) Effects of annealing temperature on the position of I $3d_{5/2}$ peak for clean and O-dosed Ru. For (B) and (D) the CH_2I_2 exposure was 6 L and θ_{O} was 0.5.

2.2. Materials

The 99.99% purity, disk-shaped Ru crystal (diameter 8 mm, thickness 1.5 mm) was oriented within 0.5° at the (001) face and was mechanically polished with diamond paste. The surface orientation was checked by XRD and LEED before mounting the sample. The crystal was spotwelded to two 0.25 mm diameter wires for resistive heating and was cooled to 110 K by conduction to a liquid nitrogen reservoir. The sample was heated from the rear by the radiation of a tungsten filament. The temperature was measured with a chromel–alumel thermocouple junction, fastened to the side of the crystal. Rigorous sample cleaning was done by Ar^+ bombardment to remove oxides and common impurities. Routine cleaning of surface was accomplished by cycling the crystal temperature between 900 and 1450 K with an O_2 flux to 1×10^{-8} mbar pressure. This was followed by annealing at 1550 K to remove adsorbed oxygen. CH_2I_2 was obtained from Fluka; it was degassed by freeze–pump–thaw cycles prior to use. The O_2 was obtained from Messer-Griesheim. $^{18}\text{O}_2$ isotope was used in TPD measurements in order to assist the identification of different oxygenated products. $^{18}\text{O}_2$ was obtained from CIL Cambridge Isotope Laboratories and it was 95–98% purity with respect to $^{16}\text{O}_2$. The oxygen coverage was determined by O 1s XPS signal which is calibrated against the ideal O coverage of $p(1 \times 2)\text{-O}$ (assumed to be 0.5 ML) [11].

3. Results

3.1. Thermal measurements

The adsorption of O_2 on Ru(001) at 110 K caused a linear increase in the work function; the maximum enhancement amounted to 1.0 eV. Exposure of O-dosed Ru to CH_2I_2 at 110 K led to a decrease of the work function by more than 1.0 eV. The final value, which was somewhat less than that of the clean Ru was attained at approximately 3.6 L of CH_2I_2 exposure (Fig. 1A). On heating the adsorbed layer, an increase in $\Delta\phi$ was observed at 200 and 300 K. The next increase

could be detected above 750 K in harmony with I desorption. Above 1000 K there was no change in $\Delta\phi$ until the O_2 desorption set in. The value (~ 0.4 eV) between 1000 and 1250 K was lower than that of the original O-dosed surface. Results obtained are plotted in Fig. 1B.

XPS spectra of O-dosed Ru in the iodine region as a function of CH_2I_2 exposure are plotted in Fig. 2A. At saturation O coverage ($\theta_{\text{O}} \approx 0.5$), a very low CH_2I_2 exposure produced an I $3d_{5/2}$ peak at 619.9 eV which shifted to higher values, up to 620.3 eV, at high exposures. Fig. 1C indicates that the uptake of CH_2I_2 on oxygen-dosed Ru(001), $\theta_{\text{O}} = 0.5$, at different CH_2I_2 exposures is practically the same as that for the clean surface. Adsorption of CH_2I_2 did not exert an observable alteration in the position of O 1s peak at 530.2 eV.

XPS spectra of coadsorbed layers annealed to different temperatures are displayed in Fig. 2B. A broadening of the I peak, indicating the onset of the dissociation of CH_2I_2 , occurred at 298 K. Above this temperature the position of the peak clearly moved to lower energy. As shown in Fig. 1D this temperature is much higher as compared with the clean surface, where a shift in the I $3d_{5/2}$ signal was detected even at 198 K [10]. A final value of the I $3d_{5/2}$ peak, 619.9 eV, corresponding to the completeness of the dissociation, is attained only at 352 K. Note that the final intensity of the I signal was almost 66% of the value measured for a clean surface.

The presence of adsorbed O markedly altered the desorption characteristics of CH_2I_2 and its decomposition products registered for a clean surface. Results obtained at $\theta_{\text{O}} = 0.25$ are shown in Fig. 3. CH_3I , detected in the products desorbing from the clean surface, was completely missing. New high temperature peaks appeared for CH_2I_2 with $T_{\text{p}} = 260$ and 298 K. The peak temperature of methane desorption also shifted from 220–230 K (clean surface) to 270 K (O-dosed surface) accompanied by a decrease in the amount of CH_4 to a low level. Smaller amounts of H_2 desorbed in several not well-resolved peaks. The most intense peaks were $T_{\text{p}} = 270$ K and $T_{\text{p}} = 490$ K. The most interesting feature is the release of new products, CH_2^{18}O ($T_{\text{p}} = 298$ K),

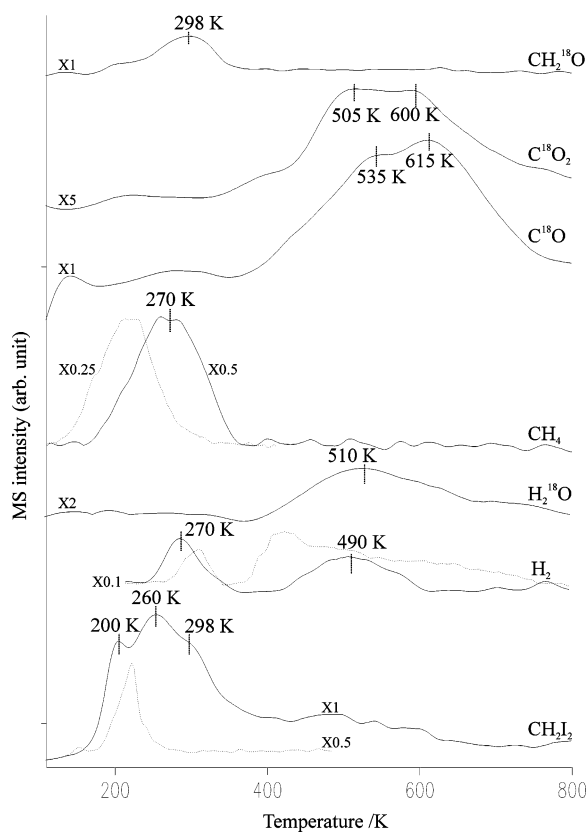


Fig. 3. Thermal desorption spectra for various products at $\theta_{\text{O}}=0.25$. CH_2I_2 exposure was 6 L. Dotted curves represent TPD products from a clean surface.

C^{18}O ($T_{\text{p}}=535$ and 615 K), C^{18}O_2 ($T_{\text{p}}=505$ and 600 K), and H_2^{18}O ($T_{\text{p}}=510$ K).

More detailed measurements on the effects of the O-coverage on the desorption of some compounds are presented in Fig. 4. A change in the desorption of CH_2I_2 occurred even at the lowest θ_{O} value, $\theta_{\text{O}}=0.06$. New desorption peaks developed at higher θ_{O} values at 250–260 and 300–340 K. The T_{p} value was 245 K for CH_2^{18}O at the lowest coverage, $\theta_{\text{O}}\approx 0.06$, which shifted to 340 K at saturation O coverage. As shown in Fig. 4C, with increasing θ_{O} value, the amount of I desorbed also decreased, and the peak temperature of iodine desorption (as I^+ species) fell from 1080 to 880 K. Interestingly, the formation of H_2^{18}O ceased above $\theta_{\text{O}}=0.25$. The peak temperatures for C^{18}O , C^{18}O_2 and H_2^{18}O did not shift with increas-

ing ^{18}O coverage, the relative amount of C^{18}O_2 increased.

Fig. 5 illustrates the effect of CH_2I_2 exposure on the desorption of CH_2I_2 and CH_2^{18}O formed at $\theta_{\text{O}}=0.5$. At low exposure, CH_2I_2 desorbed in one peak at 260 K, which shifted to lower temperature with increasing CH_2I_2 exposure. At the same time new peaks developed at 330 and 200 K. A significant change also occurred in the formation of CH_2^{18}O : its amount increased with the CH_2I_2 exposure, which was accompanied by a shift in T_{p} from 267 to 340 K (Fig. 5B). Some characteristic desorption data are collected in Table 1. Taking into account the sensitivity of the mass spectrometer to the desorbing products, we calculated that about 70% of CH_2 formed at $\theta_{\text{O}}=0.5$ was oxidized to CH_2O , and the rest was converted into a stable hydrocarbon species. As regards the product ratios we obtained, the $\text{CH}_2\text{O}/\text{CO}_2$ and $\text{CH}_2\text{O}/\text{CO}$ ratios increased monotonically as a function of O coverage.

The UP spectrum at monolayer coverage of CH_2I_2 on oxygen-dosed Ru(001) was very similar to that measured for the clean surface (Fig. 6). Photoemission lines slightly shifted to lower energies, to 4.0, 6.2, 8.7 and 13.0 eV. Significant spectral changes were experienced when the coadsorbed layer was flashed to higher temperatures. At 219 K, peaks were registered at 3.5, 5.7, 8.8 and 11.0 eV, at 298 K signals were seen at 5.0, 5.7, 8.5, 9.0 and 10.7 eV, whereas at 450 K they were at 5.4, 8.4 and 10.9 eV. Further annealing to 640 K eliminated these signals and only very weak peaks remained in the spectrum at 4.3 and 5.7 eV. Above 900 K the only detected signal was at 5.7 eV besides the characteristic photoemission lines of bare Ru metal.

3.2. Effect of illumination

The effects of photolysis of coadsorbed layer was first followed by XPS measurements. As shown in Fig. 7, a shift in the binding energy of the $\text{I } 3d_{5/2}$ signal occurred at 110 K even after a short illumination time, 1–3 min, which was independent of the O coverage. After 60 min of illumination the binding energy was at 619.7 eV, which is near the value of atomically adsorbed iodine.

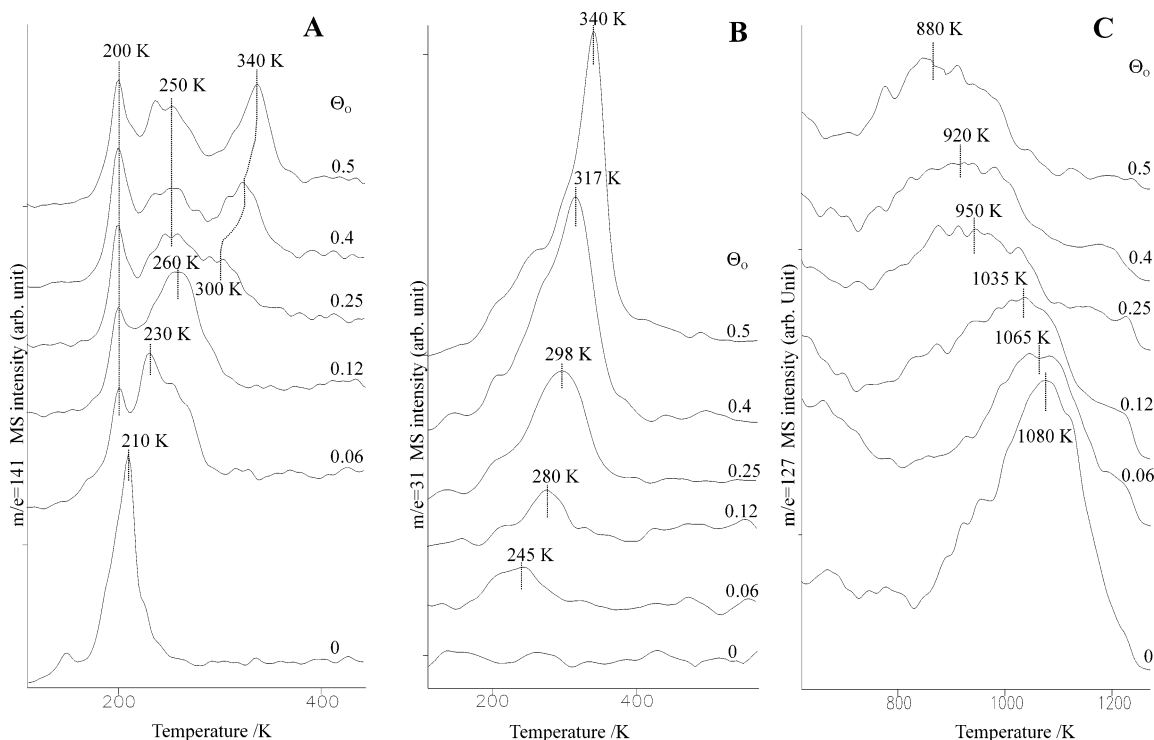


Fig. 4. Effects of O coverage on the desorption of (A) CH_2I_2 ; (B) CH_2^{18}O ; (C) I. CH_2I_2 exposure was 6 L.

The effect of photolysis at 110 K was examined with UPS method at high and low coverages of adsorbed CH_2I_2 . The He I spectra taken after illumination did not reveal the generation of CH_2 in either case. The signals of CH_2I_2 shifted to lower binding energies.

Post-irradiation TPD spectra are displayed in Fig. 8. The illumination at 110 K eliminated the low temperature peak for CH_2I_2 , and considerably decreased the amount of CH_2I_2 desorbed at higher temperature. Desorption of CH_2I_2 , however, did not cease even after 60 min of irradiation in contrast with the clean surface. Photolysis of the coadsorbed layer exerted a dramatic influence on the formation of CH_2^{18}O . Its evolution started slightly above the temperature of illumination, and after 60 min the peak temperature of its desorption was 250 K. In contrast, the temperature range of the desorption of the other products of the oxidation hardly changed (Fig. 8). A noteworthy effect is the development of a new high temperature peak for C^{18}O at 740 K, and that after 60 min of

illumination C^{18}O desorbed mainly in a peak with a $T_p = 535$ K.

4. Discussion

4.1. Adsorption and dissociation of CH_2I_2 on O-dosed Ru(001)

Previous LEED and STM measurements revealed that O atoms form islands on Ru(001) surface occupying threefold hollow sites [11]. The islands below saturation coverage are in thermodynamic equilibrium with fluctuations because of the relatively high hopping rate ($14 \pm 3 \text{ s}^{-1}$) of individual O atoms at room temperature. At $\Theta_o = 0.25$ the (2×2) structure and at saturation coverage, $\Theta_o = 0.5$, the $p(1 \times 2)$ structure were found.

XPS measurements indicate that the uptake of CH_2I_2 on oxygen-saturated Ru(001) is only slightly altered as compared with the clean surface

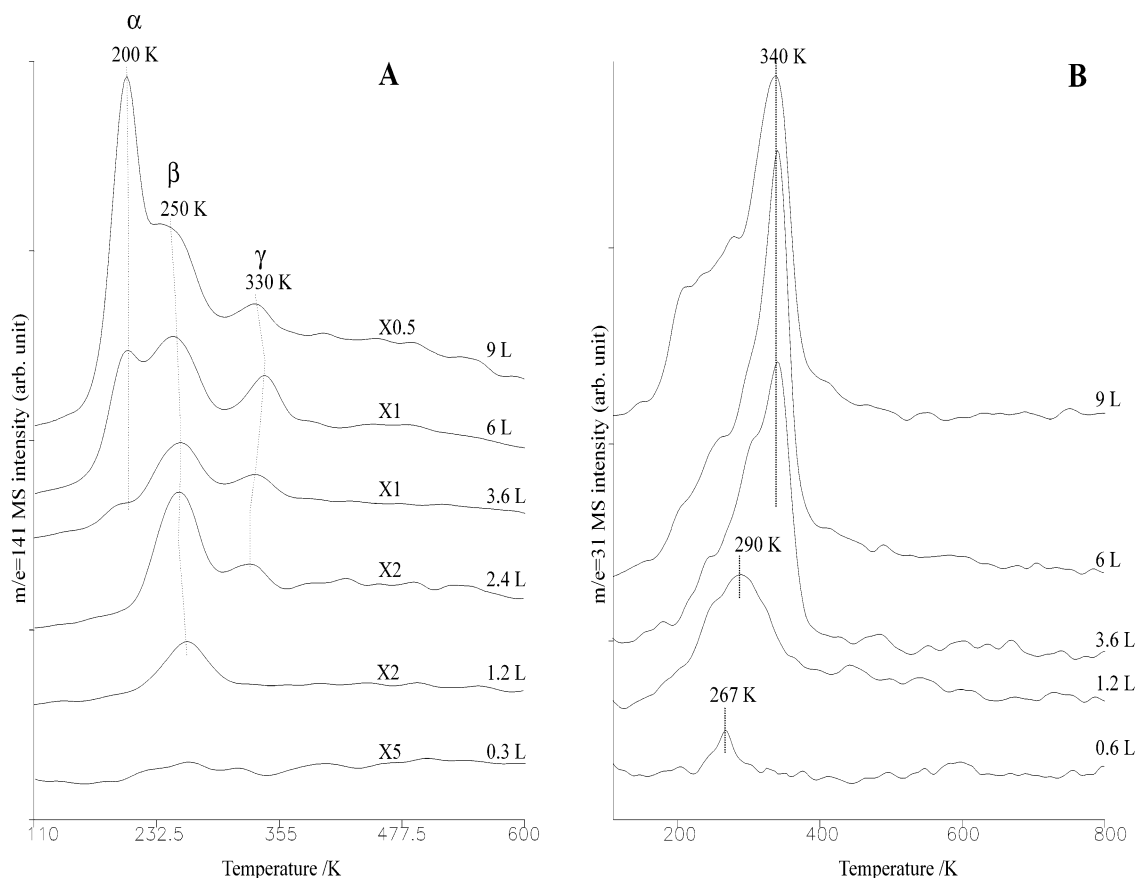


Fig. 5. Thermal desorption spectra for CH_2I_2 (A) and CH_2^{18}O (B) at $\theta_{\text{O}}=0.5$ as a function of CH_2I_2 exposure at 100 K.

Table 1

Peak temperatures for the desorption of different products following CH_2I_2 adsorption (6 L) on O-dosed Ru(001)

Desorption products	Desorption peak temperature (K)	
	$\theta_{\text{O}}=0.25$	$\theta_{\text{O}}=0.5$
CH_2I_2	200, 260, 298	200, 250, 340
CH_4	270	270
H_2	270, 490	270, 490
I^+	950	880
CH_2^{18}O	298	340
C^{18}O	535, 615	535, 615
C^{18}O_2	505, 600	520, 600
H_2^{18}O	510	510

(Fig. 1C). The position of the $\text{I } 3d_{5/2}$ peak shifted from 620.6 to 620.3 eV with increasing O coverage at approximately 1 ML coverage of CH_2I_2 indicat-

ing (i) the difference in bonding state of the molecules as compared with clean Ru(001) surface and (ii) the enhanced final state effect caused by the presence of adsorbed O atoms. The marked decrease of the work function following the adsorption of CH_2I_2 suggests that CH_2I_2 molecules – as on the clean surface – bond to the surface via their negatively charged iodine atoms (Fig. 1A). The bonding of CH_2I_2 , however, is strongly influenced by preadsorbed oxygen. The formation of a multilayer (α peak $T_p=200$ K) occurred at much lower CH_2I_2 exposure than on the clean surface (Fig. 5A), as O presumably occupies some of the bonding sites of CH_2I_2 . Its desorption temperature, however, remained unaltered. The desorption from the monolayer (designated the β peak) observed for the clean surface at $T_p=220$ K is shifted to 250 K and a new

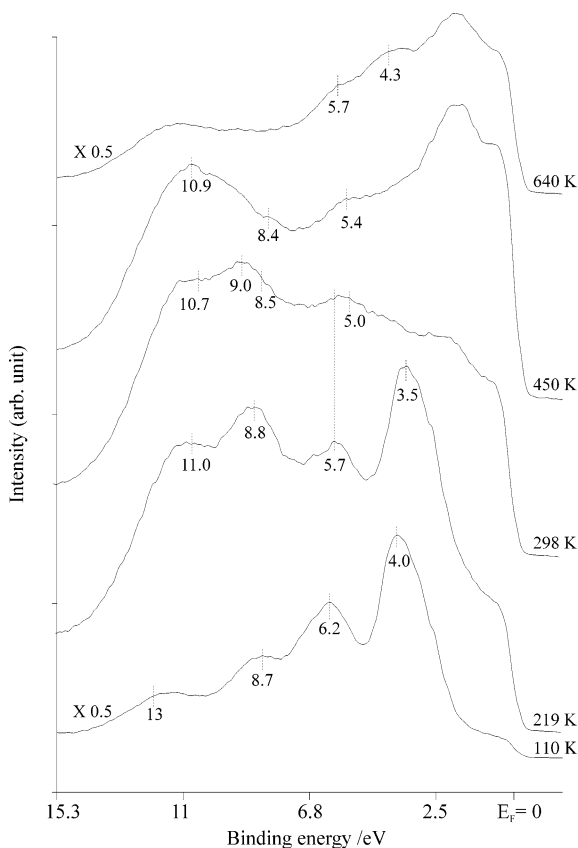


Fig. 6. He UPS spectra of Ru(001) as a function of annealing temperature at $\theta_{\text{O}}=0.5$. CH_2I_2 exposure was 6 L.

high temperature peak (γ) appeared at $T_{\text{p}}=300\text{--}350$ K. This feature indicates that CH_2I_2 is bonded close to island edges of adsorbed O, or forms $(\text{CH}_2\text{I}_2+\text{O})$ mixed island especially at high CH_2I_2 concentration. The Coulomb interaction forces between positively charged C atoms of CH_2I_2 and the negatively charged O atoms may also stabilize the CH_2I_2 molecule.

The stabilization of adsorbed CH_2I_2 is reflected in its dissociation. In the XP spectra, a shift in the binding energy of $\text{I } 3d_{5/2}$, corresponding to the dissociation of adsorbed CH_2I_2 at monolayer, occurred at higher temperatures than on a clean surface: the difference amounts to 100 K at saturation O coverage (Fig. 1D). In the explanation of these features we cannot rule out that preadsorbed oxygen atoms, by occupying the adsorption sites, prevent the dissociation of CH_2I_2 , and hence force

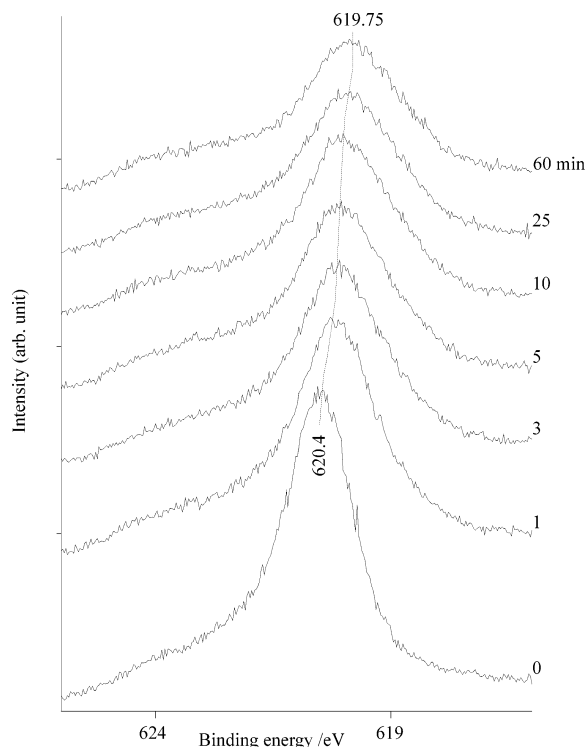


Fig. 7. Effects of illumination on the XPS spectra of adsorbed CH_2I_2 on O-dosed Ru(001) at 110 K. $\theta_{\text{O}}=0.5$. CH_2I_2 exposure was 6 L.

a fraction of adsorbed molecules to desorb instead of dissociating. We may also assume that the strong interaction between adsorbed CH_2I_2 and O also contributes to the stabilization of C–I bonds by decreasing the electron density of Ru d s bands from where electrons are donated to C–I anti-bonding orbitals. Interestingly, preadsorbed O atoms also affect the desorption of iodine: it lowers the peak temperature by almost 200 K (Fig. 4C), which we attribute to the repulsive interaction between O and I in the adsorbed layer.

The effect of preadsorbed oxygen is manifested in the reactions of CH_2 observed for the clean surface: its self-hydrogenation into methane occurred at higher temperature than on the oxygen-free surface, in accord with the higher dissociation temperature. In addition, a large fraction of CH_2 formed undergoes oxidation in the adsorbed layer, which led to the decrease in the amount of CH_4 formed. At $\theta_{\text{O}}=0.5$, CH_4 was no

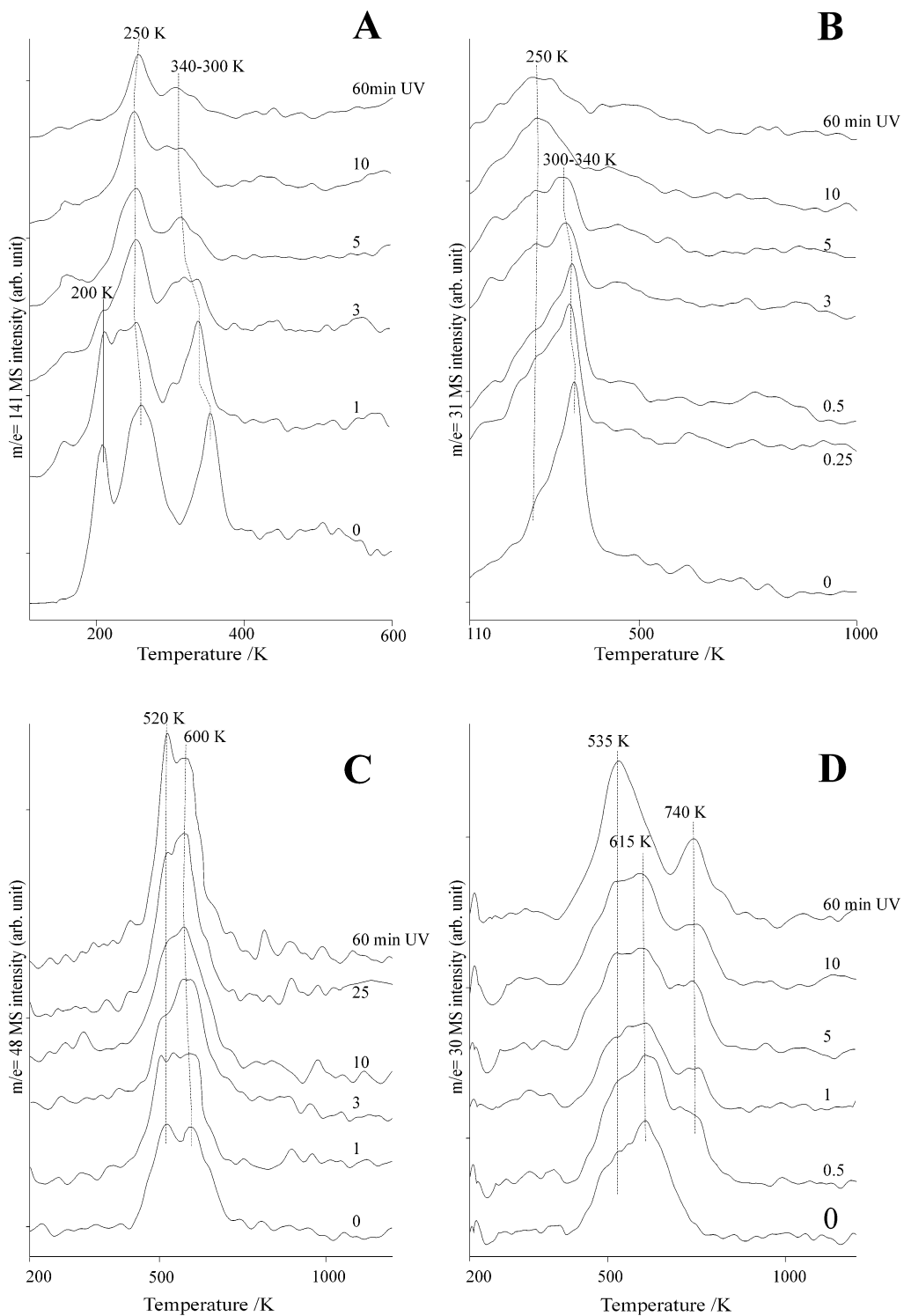


Fig. 8. Post-irradiation TPD spectra for adsorbed CH_2I_2 . (A) CH_2I_2 ; (B) CH_2^{18}O ; (C) C^{18}O_2 ; (D) C^{18}O . $\theta_{\text{O}}=0.5$. CH_2I_2 exposure was 6 L.

longer detectable in the desorbing gases. The products detected are CH_2^{18}O , H_2^{18}O , C^{18}O and C^{18}O_2 . An interesting feature of the CH_2^{18}O formation is that its peak temperature sensitively depends on the oxygen coverage (Fig. 4B). At the lowest coverage, $\theta_{\text{O}}=0.06$, CH_2^{18}O was released at $T_{\text{p}}=245$ K, while at saturation oxygen coverage, $\theta_{\text{O}}=0.5$, this value was 340 K with a tail extending below 200 K in both cases. This behavior is no doubt in connection with the inhibition of the dissociation of CH_2I_2 with increasing oxygen coverage, as indicated by the XPS results (Fig. 2). Accordingly, we may assume that the dissociation of CH_2I_2 is the prerequisite for the formation of the CH_2^{18}O , in this temperature regime. A similar conclusion was reached for the Rh(111) and Pd(100) surface [4,8]. This conclusion was confirmed by the study of the reaction of CH_2Cl_2 on O-dosed Pd(100) [8]. This compound adsorbs molecularly on Pd(100) and desorbs below 250–300 K with detectable dissociation. Following the adsorption of CH_2Cl_2 on oxygen-dosed Pd(100), we found no traces of CH_2O and detected only very small amounts of H_2O and CO_2 . However, when the adsorbed layer was illuminated – which promoted the dissociation of the C–Cl bond on Pd(100) [8] – the formation of CH_2O occurred easily.

We cannot rule out, however, that the formation of CH_2^{18}O , particularly above 300 K, proceeds as a result of a rearrangement between the strongly stabilized CH_2I_2 ($T_{\text{p}}=340$ K) and ^{18}O , as described in the scheme below:

The small FWHM value for CH_2^{18}O desorption and the coincidence of the desorption peaks of CH_2^{18}O and CH_2I_2 suggest that the formation and desorption of CH_2^{18}O in this temperature regime is controlled by the amount of strongly stabilized CH_2I_2 . Concomitant desorption requires that the

activation energy of this reaction must be higher than the energy necessary for the desorption of CH_2^{18}O .

In the study of the behavior of CH_2O on clean Ru(001), it appeared that the CH_2O desorbs from the clean Ru(001) surface in three peaks, $T_{\text{p}}=130$, 150 and 275 K [12]. The decomposition of adsorbed CH_2O occurred at 250–300 K to give H_2 and CO . On oxygen-dosed Ru(001), $\theta_{\text{O}}=0.25$, the formation of formate species was detected by HREELS which decomposed in the temperature range of 400–450 K [12]. The peak temperatures for CH_2O desorption and the products of CH_2O decomposition remained practically unaltered: neither H_2O nor CO_2 were detected in the desorbing gases. As a result of the effect of preadsorbed O, the peak temperature for CO slightly shifted to lower temperature, to 450 K [12] which is consistent with the previous results obtained for CO+O/Ru(001) system [13]. In the present case these products are released at much higher temperature, $T_{\text{p}}=505$ –615 K in two distinct peaks (Fig. 3). As H_2O and CO_2 desorb from Ru(001) below room temperature [14,15], we can conclude that the evolution of these compounds is a reaction-limited process. As the peak temperature for CO desorption from Ru(001) is 450–500 K [16], the release of a certain fraction of CO in the present case is also a reaction-limited process. As neither CH_2 nor CH_2O are stable above 600 K it seems likely that C_xH_y fragments produced by reaction of CH_2 are oxidized to the above compounds with $T_{\text{p}}=600$ –615 K. This assumption is supported by our results obtained in the oxidation of CCH_3 on clean Ru(001) where C^{18}O and C^{18}O_2 peak appeared above 600 K. The oxidation of C^{18}O formed in the decomposition of CH_2^{18}O may also contribute to the production of C^{18}O_2 . We note here that the decomposition of

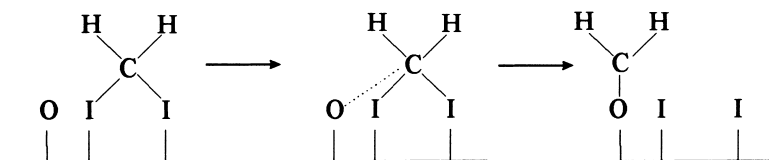


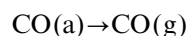
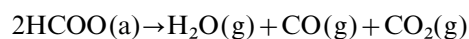
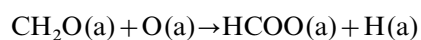
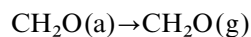
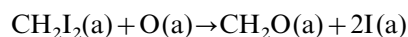
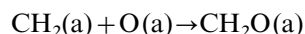
Table 2
UPS signals of various adsorbed species formed in the adsorption and reactions of CH₂I₂ on O-dosed Ru(001)

Species	Surface	Photoemission signals (eV)	Reference	Signals observed in the present work (eV)
O	Cu(100)	5.7–6.0	[8,9]	5.4
CH ₂ I ₂	Pd(100)	4.3, 6.8, 9.0, 13.0	[8,9]	4.0, 6.2, 8.7, 13.0
CH ₂	Pd(100)	5.9–6.1	[8,9]	5.7
I	Cu(100)	5.5	[9]	5.7
CH ₂ O	Cu(110)	5.7, 9.3, 11.2, 16.0	[19]	5.7, 8.8, 11.0
HCOO	K/Pd(100)	5.1–5.3, 8.6–8.9, 10.3–10.7, 13.7–13.8	[20]	5.0, 8.5, 9.0, 10.7
H ₂ O	Pd(100)	6.2, 8.5, 12.3	[8]	–
CO	Pd(100)	8.2, 10.8	[21]	8.4, 10.9

formate species on Ru(001) produced H₂, H₂O, CO and CO₂ [17,18], which is in contradiction with the previous results of the same school [12]. Accepting this finding we can also count with the occurrence of this process below 600 K.

In a search for new adsorbed compounds, UPS measurements were carried out under similar conditions. In order to assist assignment, in Table 2 we list the photoemission signals of all surface compounds possibly formed in the coadsorbed layer. On annealing the sample to 219 K (Fig. 6), new photoemission signals were seen at 5.7, 8.8 and 11.0 eV which can be attributed to adsorbed CH₂O [19]. This means that CH₂O could remain in the adsorbed layer after its formation, which was not experienced for Pd(100) and Rh(111) surfaces [4,8]. At 298 K, other new lines appeared at 5.0, 8.5, 9.0 and 10.7 eV, which can be assigned to the adsorbed HCOO species [20]. Above 450 K, the dominant photoemission peaks were at 8.4 and 10.9 eV, which are characteristic of the adsorbed CO [21].

Taking into account the above characteristics we can infer the occurrence of the following elementary steps in the oxidation of CH₂ fragments:



4.2. Photoinduced reactions in the coadsorbed layer

Post-irradiation TPD measurements clearly showed that illumination eliminated the condensed CH₂I₂ characterised with a peak temperature of 200 K (Fig. 8A). As was indicated by the XPS results, illumination of the CH₂I₂ + O coadsorbed layer markedly enhanced the dissociation of CH₂I₂ even at 110 K. A complete dissociation, however, was not achieved even after 60 min of illumination. As a result of the enhanced dissociation, a relatively large amount of adsorbed CH₂ formed at 110 K, which underwent reaction with adsorbed O atoms after its formation. This is indicated by the beginning of the release of a fraction of CH₂O slightly above the temperature of the illumination (Fig. 8B). By mean of UPS we could not detect CH₂O at 110 K, but we observed its photoemission signs above 200 K. The desorption of the other products of the oxidation, CO, CO₂ and H₂O, still occurred in the same temperature range as in the dark experiments confirming our previous conclusion that the evolution of these compounds are reaction-limited processes. A new desorption peak for C¹⁸O desorption appeared at $T_p = 740$ K (Fig. 8D), which is characteristic of oxidation of surface carbon coming from the ther-

mal decomposition of CCH_3 . This feature indicates that as a result of the larger amount of CH_2 groups produced by illumination, a fraction of CH_2 is directly decomposed to carbonaceous species, and/or transformed into C_xH_y through the formation of ethylene and ethylidyne.

5. Conclusion

1. The uptake of CH_2I_2 at 110 K was not influenced by adsorbed O atoms.
2. Preadsorbed O atoms significantly stabilize the C–I bond, shift its dissociation temperature by 100 K to higher temperature and caused the formation of a new adsorbed state.
3. Oxygen atoms coupled with CH_2 , the dissociation product of CH_2I_2 , above 200 K to give CH_2O . At higher temperature the formation of formate species also occurred.
4. The oxidation of C_xH_y fragments and decomposition products of formaldehyde and formate proceeded above 450 K to yield H_2O , CO and CO_2 .
5. Illumination enhanced the extent of dissociation of CH_2I_2 , and even at 110 K caused the formation of formaldehyde slightly above this temperature.

Acknowledgement

This work was supported by the Hungarian Academy of Sciences and Grants OTKA T23023.

References

- [1] F. Solymosi, *J. Mol. Catal.* 131 (1998) 121.
- [2] X.Y. Zhou, Z.M. Liu, J. Kiss, D.W. Sloan, J.M. White, *J. Am. Chem. Soc.* 117 (1995) 3565.
- [3] F. Solymosi, Paper presented at the IUUVSTA workshop on 'The Structure and Reactivity of Small Molecules on Surfaces', Brdo, April 9–15, 1995.
- [4] F. Solymosi, G. Klivényi, *J. Phys. Chem.* 99 (1995) 8950.
- [5] G. Klivényi, F. Solymosi, *Surf. Sci.* 342 (1995) 168.
- [6] C.W.J. Bol, C.M. Friend, *J. Am. Chem. Soc.* 117 (1995) 11 572.
- [7] C.W.J. Bol, C.M. Friend, *Surf. Sci. Lett.* 337 (1995) L800.
- [8] F. Solymosi, I. Kovács, K. Révész, *Surf. Sci.* 356 (1996) 121.
- [9] I. Kovács, F. Solymosi, *J. Mol. Catal. A: Chem.* 141 (1999) 31.
- [10] A. Kis, K.C. Smith, J. Kiss, F. Solymosi, *Surf. Sci.* (2000) in press.
- [11] J. Wintterlin, J. Trost, S. Renisch, R. Shuster, T. Zambelli, G. Ertl, *Surf. Sci.* 394 (1996) 159.
- [12] A.B. Anton, J.E. Parmeter, W.H. Weinberg, *J. Am. Chem. Soc.* 108 (1986) 1823.
- [13] F. Buatier de Mongert, M. Scherer, B. Gleich, E. Kopatzki, R.J. Behm, *Surf. Sci.* 411 (1998) 249.
- [14] P.K. Leavit, J.L. Davis, J.S. Dyer, P.A. Thiel, *Surf. Sci.* 218 (1989) 346.
- [15] F.H. Hoffmann, M.D. Wiesel, J. Paul, *Surf. Sci.* 316 (1994) 277.
- [16] H. Pfnür, P. Feulner, D. Menzel, *J. Chem. Phys.* 79 (1983) 2400.
- [17] M.D. Weisel, J.G. Chen, F.H. Hoffmann, Y.K. San, W.H. Weinberg, *J. Chem. Phys.* 97 (1992) 9396.
- [18] B. Meng, T.A. Jachimowski, Y. San, W.H. Weinberg, *Surf. Sci.* 315 (1984) L959.
- [19] B.A. Sexton, A.E. Hughes, N.R. Avery, *Surf. Sci.* 155 (1985) 366.
- [20] F. Solymosi, I. Kovács, *Surf. Sci.* 259 (1991) 95.
- [21] F. Solymosi, A. Berkó, Z. Tóth, *Surf. Sci.* 285 (1993) 197.